# An Enhanced MMSE Subchannel Decision Feedback Equalizer with ICI Suppression for FBMC/OQAM Systems

Chih-Wei CHEN and Fumiaki MAEHARA
Graduate School of Fundamental Science and Engineering, Waseda University
3-4-1 Okubo, Shinjuku-ku, Tokyo 169-8555, Japan
Email: cvsi04236@fuji.waseda.jp

***Abstract*— This paper proposes an enhanced decision feedback equalizer (DFE) for filter bank multicarrier (FBMC) systems over offset quadrature amplitude modulation (OQAM) based on a minimal mean square error (MMSE) criterion. For each subcarrier, besides one feedforward (FF) filter and one feedback (FB) filter, we add two intercarrier interference (ICI)-suppressing filters, which feed back detected precursors extracted from neighboring subchannels to enhance ICI suppression in the presence of multipath channels. Our simulation results indicate our proposal makes a considerable improvement comparing with MMSE-DFE under a severe ICI and ISI scenario despite few extra costs in computational complexity.**

*Keywords*–FBMC, OQAM, MMSE, decision feedback equalizer, intercarrier interference

## I. INTRODUCTION

Nowadays, multicarrier (MC) systems are widely-known and attractive for wideband communications. The most well-known system is orthogonal frequency-division multiplexing (OFDM), which encodes digital data on many narrowly-divided frequency subbands. The advantages of OFDM include simple equalization, channel estimation and the ability to combat severe channel conditions such as frequency-selective fading [1]. OFDM recently has several applications, including digital television, audio broadcasting and 4G mobile communications. However, the orthogonality between OFDM subcarriers is maintained by adding cyclic prefixes (CP), which are the replicas of tailed signals of OFDM [2]. CP delimit successive OFDM symbols and bring about block transmission of OFDM, but sending CP certainly lowers power efficiency and data rate. In addition, sensitivity in frequency offset and out-of-band interference are two other problems in OFDM. To cope with these problems of OFDM, some people discuss about FBMC that can be viewed as a practical alternative to OFDM.

FBMC is also a MC system and subcarriers in filter banks are exponentially composed with longer impulse responses than OFDM signals [3]. Compared to rectangular prototype signals of OFDM, longer impulse responses of FBMC subcarriers enable FBMC to control non-adjacent orthogonality between FBMC subcarriers. As a consequence, the well-controlled orthogonality relieves out-of-band interference and frequency sensitivity of FBMC. Meanwhile, without redundant CP, FBMC can support higher power efficiency and throughput, and successive transmission can be achieved since block structure disappears. Additionally, to dodge ISI coming from overlapped FBMC signals and ICI between adjacent subcarriers, a novel OQAM scheme is used in FBMC. OQAM modulation staggers real parts and imaginary parts of QAM inputs to have adjacent subcarriers carry out-of-phase half symbols simultaneously. In spite of it, when facing ISI channels, ISI and ICI still exist. In addition to additive white Gaussian noise (AWGN) at receivers, equalizer designs become a popular topic [4].

In [5], the authors illustrate a solution to the equalization problem, but the solution is approximated by the steepest descent algorithm instead of a closed form. An extension of [5] is proposed in [6], where the equalizer is equipped with three filters for each subcarrier. The authors of [7] firstly present an MMSE linear equalizer for each subcarrier and based on [7], a two-stage (TS)-MMSE and an MMSE-DFE are proposed in [8] and [9]. The TS-MMSE is able to accomplish full ICI cancellation but its requirements for information of postcursors cause an additional latency in equalization. In [9], an extra FB filter is cascaded to enhance ISI suppressing and the improvement is shown but there is still a room to improve ICI suppression.

Considering the background, we proposed an enhanced DFE structure to suppress not only ISI but ICI all at once. Based on a MMSE criterion and taking MMSE-DFE in [9] as a prototype, we add two additional ICI suppressing filters to feed back detected precursors of adjacent subcarriers and in so doing, improvement in eliminating interference can be expected. To confirm the effectiveness, we evaluate our proposal and previous works of MMSE and MMSE-DFE in terms of computational complexity and bit-error-rate (BER).

An introductory explanation of FBMC/OQAM is in Section II, and Section III elaborates upon the proposed equalizer design. Performance evaluations are shown in Section IV, then followed by the conclusions.

### A. Notation

In this paper, we use the following notations for convenience. $(\bullet)^{(\mathrm{R})}$ and $(\bullet)^{(\mathrm{I})}$ are the real part and imaginary part of a signal or a vector. $j$ is $\sqrt{-1}$. A notation in bold is always a vector containing a finite-length sequence of symbols. $\mathbf{I}_N$ denotes the identity matrix of size $N$ and $\mathbf{0}_M$ and $\mathbf{0}_{M\times N}$ represent an $M \times 1$ and an $M \times N$ zero matrix respectively, and $\mathtt{mod}$ is the modulo operation. $\lfloor\ \rfloor$ = the flooring function, $*$ is the convolution operation.

978-1-5090-4588-4/17/$31.00 ©2017 IEEE

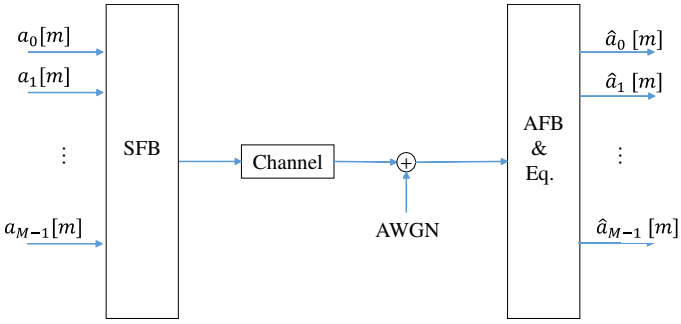


Fig. 1. Overview of FBMC

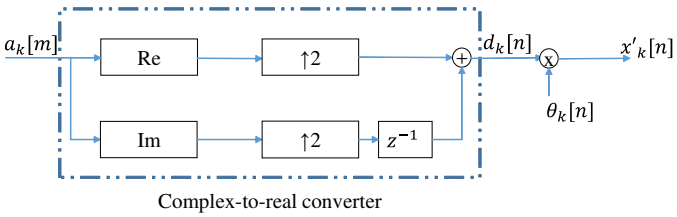


Fig. 2. OQAM pre-processing for an even $k$

## II. FBMC/OQAM STRUCTURE

The core of FBMC systems is synthesis filter banks (SFB) and analysis filter banks (AFB) as Fig. 1 shows. The inputs $a_k[m]$ are complex QAM symbols to be carried by each subcarrier. To compose OQAM symbols, OQAM pre-processing is conducted in SFB, in which real parts and imaginary parts of QAM inputs are separated as shown in Fig. 2 for an even $k$. The order of transmission for half symbols depends on the subcarrier index, $k$. For odd-index subcarriers, imaginary parts are ordered ahead by placing the one-tap delay in Fig. 2 upside down. The staggered outputs are denoted by $d_k[n]$ and then the complex OQAM symbols and denoted by $x'_k[n] = \theta_k[n]d_k[n]$ with $\theta_k[n] = j^{(n+k)\text{mod}2}$, at the double rate of the inputs. Afterwards, the OQAM symbols are upsampled by $M/2$ and fed into a bank of $M$ synthesis filters, whose impulse responses are designed by

$$h_k[l] = h_0[l]e^{\frac{j2\pi kl}{M}}, l = 0, ...KM-1. \quad (1)$$

In (1), $h_0[l]$ is the $KM$-tap causal impulse response of a prototype filter, each subcarrier is shifted by $1/M$ in frequency, and $K$ is the overlapping factor. $h_0[l]$ needs designing as a Nyquist filter to provide an ISI-free transmission, and $K$ is the ratio between the length of $h_0[l]$ and the averaged symbol duration. After filtered by SFB, all signals are composed into one waveform, up-converted into a radio frequency, and emitted. At FBMC receivers, AFB decompose down-converted signals with a bank of analysis filters. The impulse responses of AFB can be designed the same as SFB to perform the conjugated frequency responses [4]. After decomposition by AFB, received signals are downsampled, equalized and then converted into complex OQAM symbols by OQAM post-processing. A combination of OQAM post-processing and the proposed DFE is in the next section.

## III. ENHANCED SUBCHANNEL MMSE-DFE WITH ICI SUPPRESSION

In the following, we consider a FBMC system with $K \geq 4$ such that the prototype filter possesses strong controllability in its stop-band. Accordingly, the interference from non-neighboring subcarriers can be neglected. In this way, a subchannel model for the FBMC system can be drawn as Fig. 3 shows. In Fig. 3, we define $q_{k,k+j}[n]$ $(j = -1, 0, 1)$ as the effective ICI channels from the $k+j$-th carrier to the $k$-th carrier, which can be formulated by

$$q_{k,k+j}[n] = \{h_{k+j}[l] * h_{ch}[l] * h_k[l]\}|_{l=\frac{Mn}{2}}, n = 0, ..., Q-1, \quad (2)$$

where $Q = \left\lfloor \frac{2KM+L_{ch}-2}{M/2} \right\rfloor$. Then, an received $N \times 1$ vector $\mathbf{y}_k[n]$ can be analyzed in a matrix form,

$$\mathbf{y}_k[n] = \sum_{j=-1}^{1} \mathbf{Q}_{k,k+j}\mathbf{x}'_{k+j}[n] + \mathbf{\Gamma}_k\mathbf{v}[l], \quad (3)$$

In (3), $\mathbf{Q}_{k,k+j}$ are the convolutional matrixes $\in \mathbb{C}^{N\times(L+1)}$ for $q_{k,k+j}[n]$, and $\mathbf{x}'_{k+j}[n]$ are $(L+1)\times 1$ transmitted symbol vectors, where $L = N - Q - 2$. The noise vector, $\mathbf{v}[l]$ is an $(KM + \frac{NM}{2} - 1)$-tuple AWGN vector with the $k$-th downsampling convolutional matrix, $\mathbf{\Gamma}_k$ resulting from $h_k[l]$. It is worth mentioning that the phases of elements in $\mathbf{x}'_k[n]$ depends on $k+n$,

$$\mathbf{x}'_k[n] = [d_k[n]\theta_k[n], d_k[n-1]\theta_k[n-1], ...]^T \in \mathbb{C}^{L+1}. \quad (4)$$

The proposed structure of an enhanced subchannel MMSE DFE with ICI suppression is shown in Fig. 4. Firstly, as with MMSE-DFE, one FF filter $\mathbf{w}_k$ and one FB filter $\mathbf{f}_{k,k}$ are employed to filter downsampled symbols and detected symbols in the $k-th$ subchannel respectively. In addition, the main extension of our proposal is the two ICI-suppressing filters, $\mathbf{f}_{k-1,k}$, and $\mathbf{f}_{k+1,k}$. Once inputs of the FF filters, $\mathbf{y}_k[n]$ are filtered, they are subtracted by the outputs of the three FB filters. The contribution of the FB filter $\mathbf{f}_{k,k}$ lies in the ISI suppression, so called the ISI-suppressing filter. In contrast, $\mathbf{f}_{k-1,k}$ and $\mathbf{f}_{k+1,k}$ serve as ICI-suppressors that extract the detected symbols from adjacent subcarriers to strengthen ICI suppression. The former and latter indexes in FB filters indicate FB sources and destinations respectively. After subtraction, a detector and OQAM post-processing are followed to restore OQAM symbols and generate the latest FB inputs as Fig. 5 shows. For an odd-index subcarrier, the multiplication with $j$ is placed upside down to match the order of transmission. The input vectors of the FB filters, denoted by $\hat{\mathbf{x}}_{k+j}[n]$ with $B+1$ tuples are real-valued vectors and defined by

$$\hat{\mathbf{x}}_{k+j}[n] = [d_{k+j}[n-\mu-1], d_{k+j}[n-\mu-2], ...]^T \in \mathbb{R}^{B+1} \quad (5)$$

where all the detections of precursors are assumed to be correct. The value $\mu$ is a proper delay for equalization, which is relevent to the positions of maximum values of $h_{ch}[l]$ and $h_0[l]$ and can be optimized by simulation. In this paper, we set $\mu$ as a multiple of two but do not

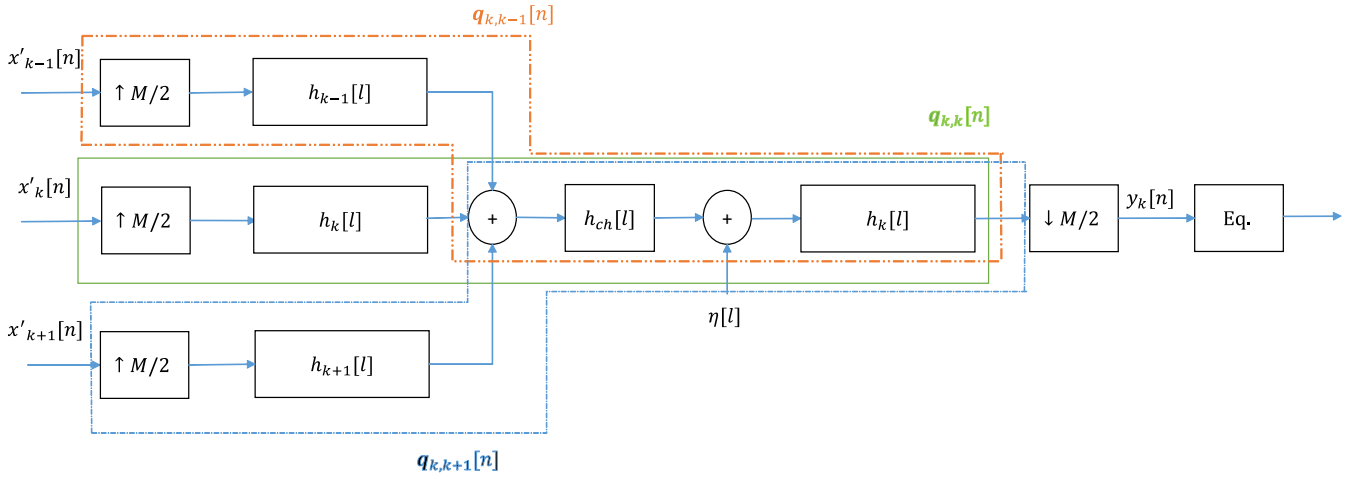


Fig. 3. Subchannel model for the $k$-th subcarrier

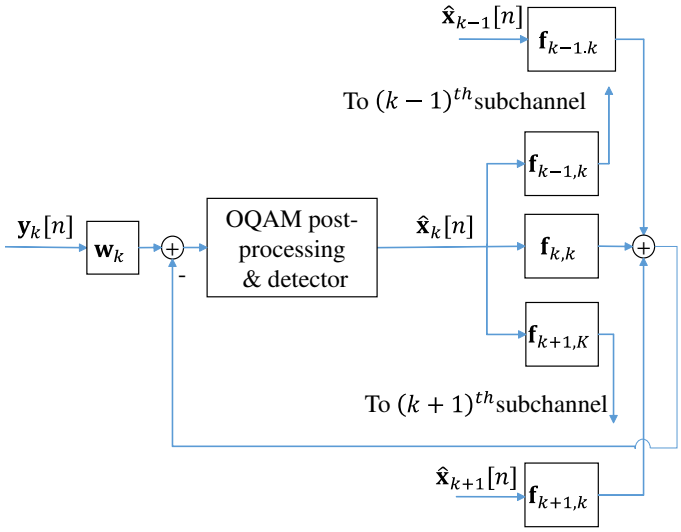


Fig. 4. Enhanced DFE with ICI suppressing filters

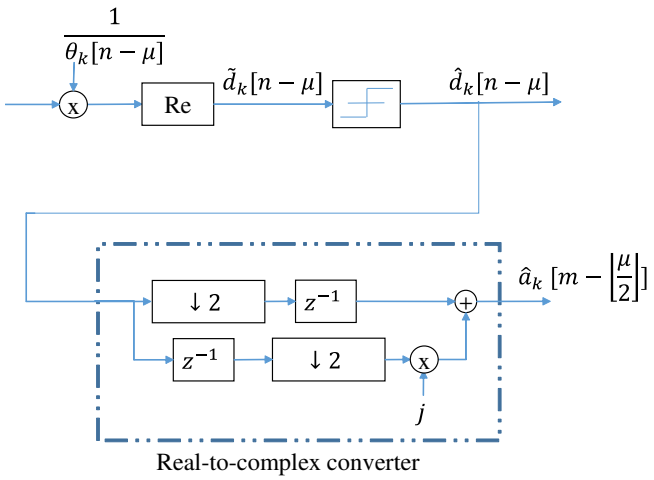


Fig. 5. OQAM pre-processing and detector

deal with the optimization. Instead, we use a fix value for $\mu$ through all simulations. Notably, when the detection of $d_{k+j}[n-\mu]$ is finished, the FB vectors are updated by pushing in $d_{k+j}[n-\mu]$.

Next, when estimating $d_k[n-\mu]$ for an even $n+k$, since the desired symbol is real-valued, the estimate, denoted by $\tilde{d}_k[n-\mu]$, can be expressed by

$$\tilde{d}_k[n-\mu] = \left[\mathbf{w}_k^H \mathbf{y}_k[n] - \sum_{j=-1}^{1} \mathbf{f}_{k+j,k}^H \hat{\mathbf{x}}_{k+j}[n]\right]^{(\mathrm{R})}$$

$$= \mathbf{w}_k^{(\mathrm{R}),T} \mathbf{y}_k^{(\mathrm{R})}[n] + \mathbf{w}_k^{(\mathrm{I}),T} \mathbf{y}_k^{(\mathrm{I})}[n] - \sum_{j=-1}^{1} \mathbf{f}_{k+j,k}^{(\mathrm{R}),T} \hat{\mathbf{x}}_{k+j}[n]. \quad (6)$$

As for an odd $(n+k)$, the estimate is given by

$$\tilde{d}_k[n-\mu] = \left[\mathbf{w}_k^H \mathbf{y}_k[n] - \sum_{j=-1}^{1} \mathbf{f}_{k+j,k}^H \hat{\mathbf{x}}_{k+j}[n]\right]^{(\mathrm{I})}$$

$$= \mathbf{w}_k^{(\mathrm{R}),T} \mathbf{y}_k^{(\mathrm{I})}[n] - \mathbf{w}_k^{(\mathrm{I}),T} \mathbf{y}_k^{(\mathrm{R})}[n] + \sum_{j=-1}^{1} \mathbf{f}_{k+j,k}^{(\mathrm{I}),T} \hat{\mathbf{x}}_{k+j}[n]. \quad (7)$$

In the above two equations, the real and imaginary parts of received symbols can be rewritten by

$$\mathbf{y}_k^{(\mathrm{R})}[n] = \left[\sum_{j=-1}^{1} \mathbf{Q}_{k,k+j} \mathbf{x}'_{k+j}[n] + \mathbf{\Gamma}_k \mathbf{v}[l]\right]^{(\mathrm{R})}$$

$$= \sum_{j=-1}^{1} \mathbf{Q}'^{(\mathrm{R})}_{k,k+j} \mathbf{x}_{k+j}[n] + \mathbf{\Gamma}_k^{(\mathrm{R})} \mathbf{v}^{(\mathrm{R})}[l] - \mathbf{\Gamma}_k^{(\mathrm{I})} \mathbf{v}^{(\mathrm{I})}[l], \quad (8)$$

$$\mathbf{y}_k^{(\mathrm{I})}[n] = \left[\sum_{j=-1}^{1} \mathbf{Q}_{k,k+j} \mathbf{x}'_{k+j}[n] + \mathbf{\Gamma}_k \mathbf{v}[l]\right]^{(\mathrm{I})}$$

$$= \sum_{j=-1}^{1} \mathbf{Q}'^{(\mathrm{I})}_{k,k+j} \mathbf{x}_{k+j}[n] + \mathbf{\Gamma}_k^{(\mathrm{I})} \mathbf{v}^{(\mathrm{I})}[l] + \mathbf{\Gamma}_k^{(\mathrm{I})} \mathbf{v}^{(\mathrm{R})}[l], \quad (9)$$

where $\mathbf{x}_{k+j}[n] \in \mathbb{R}^L$ are obtained by shifting all $j$'s from $\mathbf{x}'_{k+j}[n]$ to $\mathbf{Q}_{k,k+j}$ to recover a staggered form matching with

$\hat{\mathbf{x}}_{k+j}[n]$, resulting in the matrixes $\mathbf{Q}'_{k,k+j}$ that contain the effect of $\theta_k[n]$, SFB, channels, AFB. For an even $k+n$, in all $\mathbf{Q}'_{k,k+j}$, the dimensions are unchanged but all the multiple-of-two-index columns are multiplied by $j$. Then, by defining the error as the distance between the estimate and the desired symbol, the MMSE criterion can be defined by

$$\begin{bmatrix} \mathbf{w}_{k,o} \\ \mathbf{f}_{k,FB,o} \end{bmatrix} = \arg \min_{\mathbf{w}_k, \mathbf{f}_{k,FB}} \mathrm{E}[|d_k[n-\mu] - \tilde{d}_k[n-\mu]|^2], \quad (10)$$

where $\mathbf{f}_{k,FB} = [\mathbf{f}_{k,k}^T, \mathbf{f}_{k-1,k}^T, \mathbf{f}_{k+1,k}^T]^T$. If $d_k[m]$ are wide-sense stationary and uncorrelated, (6) and (7) can be optimized individually. Obviously, solving (6) only leads to the real part the MMSE solution of $\mathbf{f}_{k,FB}$ because the inputs of the FB filters are real, while solving (7) leads to the imaginary part. Since we can prove that for a fixed $k$, the MMSE solutions for $\mathbf{w}'_{k,o}$ from (6) and (7) are the same, and for FB filters, $\mathbf{f}^{(\mathrm{R})}_{k,k,o}[n] = (-1)^n \mathbf{f}^{(\mathrm{I})}_{k,k,o}[n]$ and $\mathbf{f}^{(\mathrm{R})}_{k,k\pm1,o}[n] = (-1)^{(n+1)} \mathbf{f}^{(\mathrm{I})}_{k,k\pm1,o}[n]$, the above operations on $\mathbf{Q}_{k,k+j}$ can be performed to obtain the following solutions in every subchannel.

With the above analysis, we assume that the variance of AWGN is $\sigma_\eta^2$ and $\mathrm{E}[|d_k[n]|^2] = \sigma_d^2/2$. By plugging (8) and (9), into (6) and (7) and with the orthogonality principle from (10), $\mathrm{E}[\epsilon_k[n]\mathbf{y}'_k[n]] = \mathbf{0}_{2N+3(B+1)}$, where $\epsilon_k[n] = d_k[n-\mu] - \tilde{d}_k[n-\mu]$, and $\mathbf{y}'_k[n] = \left[\mathbf{y}_k^{(\mathrm{R}),T}[n], \mathbf{y}_k^{(\mathrm{I}),T}[n], -\hat{\mathbf{x}}_k^T[n], -\hat{\mathbf{x}}_{k-1}^T[n], -\hat{\mathbf{x}}_{k+1}^T[n]\right]^T$, and with the definition of $\mathbf{w}'_k = [\mathbf{w}_k^{(\mathrm{R}),T}, \mathbf{w}_k^{(\mathrm{I}),T}]^T \in \mathbb{R}^{2N}$, the MMSE solution, (8) concludes with

$$\begin{bmatrix} \mathbf{w}'_{k,o} \\ \mathbf{f}^{(\mathrm{R})}_{k,FB} \end{bmatrix} = \begin{bmatrix} \mathbf{H}_k\mathbf{H}_k^T + \mathbf{M}_k\mathbf{M}_k^T + \mathbf{N}_k\mathbf{N}_k^T + \mathbf{R}_{\eta,k} & -\frac{\sigma_d}{\sqrt{2}}\mathbf{F}_k\mathbf{J}_\mu \\ -\frac{\sigma_d}{\sqrt{2}}(\mathbf{F}_k\mathbf{J}_\mu)^T & \frac{\sigma_d^2}{2}\mathbf{I}_{3(B+1)} \end{bmatrix}^{-1} \begin{bmatrix} \frac{\sigma_d}{\sqrt{2}}\mathbf{H}_k\mathbf{e}_\mu \\ \mathbf{0}_{3B+3} \end{bmatrix} \quad (11)$$

with the following definitions, $\mathbf{F}_k = [\mathbf{H}_k, \mathbf{M}_k, \mathbf{N}_k]$, $\mathbf{H}_k = \frac{\sigma_d}{\sqrt{2}}\begin{bmatrix} \mathbf{Q}'^{(\mathrm{R})}_{k,k} \\ \mathbf{Q}'^{(\mathrm{I})}_{k,k} \end{bmatrix}$, $\mathbf{M}_k = \frac{\sigma_d}{\sqrt{2}}\begin{bmatrix} \mathbf{Q}'^{(\mathrm{R})}_{k-1,k} \\ \mathbf{Q}'^{(\mathrm{I})}_{k-1,k} \end{bmatrix}$, $\mathbf{N}_k = \frac{\sigma_d}{\sqrt{2}}\begin{bmatrix} \mathbf{Q}'^{(\mathrm{R})}_{k+1,k} \\ \mathbf{Q}'^{(\mathrm{I})}_{k+1,k} \end{bmatrix}$ $\mathbf{R}_{\eta,k} = \frac{\sigma_\eta^2}{2}\mathbf{\Gamma}'_k\mathbf{\Gamma}'^T_k, \mathbf{\Gamma}'_k = \begin{bmatrix} \mathbf{\Gamma}^{(\mathrm{R})}_k & \mathbf{\Gamma}^{(\mathrm{R})}_k \\ \mathbf{\Gamma}^{(\mathrm{I})}_k & -\mathbf{\Gamma}^{(\mathrm{I})}_k \end{bmatrix}$, and $\mathbf{J}_\mu$ is an $(L+1)\times(B+1)$ matrix whose value is defined according to $L, \mu$ and $B$,

$$\mathbf{J}_\mu = \begin{cases} [\mathbf{0}_{(\mu+1)\times B'}\mathbf{I}_{B'}\mathbf{0}_{(L-B'-\mu)\times B'}]^T, L-\mu > B', \\ [\mathbf{0}_{(\mu+1)\times B'} \ \overset{\mathbf{I}_{B'}}{\underset{\mathbf{0}_{(L-\mu)\times(B'+\mu-L)}}{}} \ ]^T, L-\mu < B', \\ [\mathbf{0}_{(\mu+1)\times B'}\mathbf{I}_{B'}]^T, L-\mu = B', \end{cases} \quad (12)$$

where $B' = B+1$.

## IV. Performance evaluations

In this section, to contrast our proposal and the former works, including one-tap, MMSE, and MMSE-DFE, we discuss their structural configurations and corresponding computational complexity first. Then we show our simulation results to confirm their effectiveness and performance.

TABLE I
Complexity analysis. Design complexity and processing complexity for each design

| | Design Complexity | Processing Complexity |
|---|---|---|
| One-tap | 0 | 2 |
| MMSE | $O(N^2)$ | $2N$ |
| MMSE-DFE | $O(N^2+NB+B^2)$ | $2N+B+1$ |
| Our proposal | $O(N^2+NB+B^2)$ | $2N+3B+3$ |

### A. Complexity analysis

Firstly, all of the equalizers are equipped with a FF filter. A one-tap equalizer provides the simplest solution with an unit-tap filter; in contrast, the other three equalizers supply an $N$-tap FF filter. MMSE-DFE and our enhanced DFE have extra FB structure to combat ISI and ICI. MMSE-DFE has one $B+1$-tap FB filter and our proposal has three.

We consider complexity from two different points of view: design complexity and processing complexity. Firstly, since all of the MMSE-based designs mainly depend on the orthogonality principle, which turns out a cross-correlation matrix times the inverse of an auto-correlation matrix (c.f. (11)) which is the main load in designing. The complexity of an inverse operation is usually considered over $O(C^2)$ where $C^2$ is the size of the matrix. From this perspective, with all the information in those matrixes calculated in advanced, the design complexity of the above equalizers follows the matrix size.

Secondly, since only one phase is cared in each detection, we consider processing complexity in terms of the number of real multipliers (RMUX) demanded by each design. A FF and a FB filter need $2N$ and $B+1$ RMUX respectively. In contrast with MMSE-based equalizers, matrix computation is waived and only two RMUX are needed in an one-tap equalizer. Table I concludes the above analysis.

### B. BER performance

Next, we evaluate the performance of different equalizers in terms of BER. The parameter settings of the system are as follows: $M = 128$ and QPSK-modulated. The prototype filter is a root raised cosine filter with roll-off factor $= 0.5$ and the overlapping factor $K = 4$, which is a nearly Nyquist filter, such that its non-adjacent ICI can be negligible. The signal-to-noise power ratio (SNR) is defined as $\sigma_d^2/\sigma_\eta^2$. The multipath channel, $h_{ch}[n]$ follows an exponentially-decaying profile and is chosen randomly and perfectly estimated without any channel coding. In all realizations, the equalizer delay $\mu$ is eight.

Fig. 6 contrasts the performance of one-tap, MMSE, MMSE-DFE, and our proposal as a function of SNR. The maximal delay spread, $\tau_{max}$ of the channel is 25-tap and the root-mean-square (RMS) delay spread, $\tau_{rms}$ is two-tap both at the same rate of $l$. Firstly, we set all the FF filters three-tap in MMSE, MMSE-DFE and our proposal, and FB filters are two-tap (i.e., $B = 1$). As can be seen, all algorithms perform almost the same in the low SNR region (around

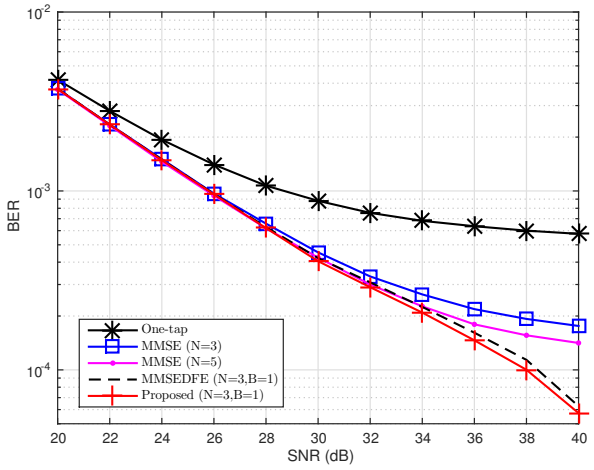


Fig. 6. BER curves of different equalizers with a varying SNR, $\tau_{max} = 25$ and $\tau_{rms} = 2$

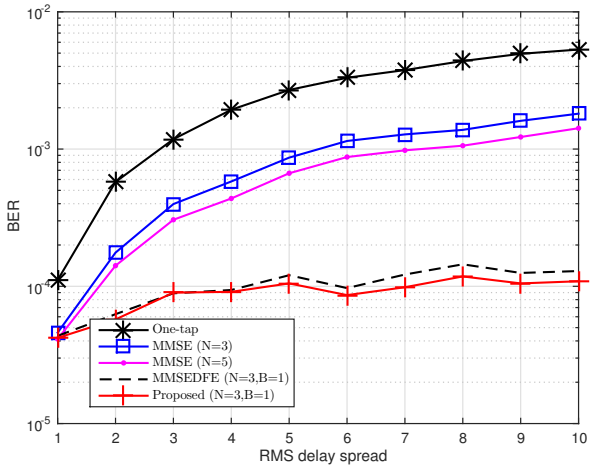


Fig. 7. BER curves of different equalizers in multipath channels with a varying $\tau_{rms}$ and SNR$= 40$ dB $\tau_{max} = 25$

20 dB). On the other hand, at the BER of $2\text{x}10^{-4}$, the ISI-suppressing filter brings a three-dB gain in SNR. Moreover, our proposal with two ICI-suppressing filters cascaded can futher improve the BER by one more dB. Even though we increase the taps of the FF filter of MMSE by two to have complexity similar to our proposal, the performance is still limited. The main reason for the limited improvement is that ISI and ICI dominate at a high SNR and the power of one FF filter of MMSE is insufficient to combat ISI and ICI. With the help of one FB filter in MMSE-DFE, ISI can be suppressed but residual ICI still remains. Our proposed ICI suppressing filters are proven capable of coping with residual ICI. In Fig. 7, we vary $\tau_{rms}$ from one tap to 10 taps and fix the SNR $= 40$ dB and $\tau_{max} = 25$. With a longer delay spread (that is, highly frequency selective), the effect of ICI and ISI becomes more outstanding as mentioned. In this simulation, we can see the three MMSE-based equalizers have similar performance at a short $\tau_{rms}$. Contrarily, our proposal outperforms the other three equalizers when $\tau_{rms}$ is increased. For the above results, we can conclude our proposed scheme can be seen as a powerful equalizer in a highly selective channel or at a high SNR.

## V. CONCLUSIONS

In conclusion, firstly, the problem of FBMC/OQAM under ISI channels is investigated. Next, using MMSE-DFE as a prototype, we propose an enhanced DFE with two ICI suppressing filters added and then optimize these filters based on the MMSE criterion. Under an error-free-detection assumption, the analytical result can be obtained. In our simulation, the improvement from the two ICI suppressing filters is considerable in a high SNR region and on highly selective channel conditions in spite of an extra slight burden in computation.

In a non-static channel, the filter coefficients need updating such that design complexity becomes more significant. Effective adaptive DFE designs like [10] are necessary in successively transmission of FBMC/OQAM. Also, erroneous FB signals need be taken into consideration. A further improvement can be expected when a selective decision feedback technique is found. Channel estimation in FBMC is also another issue.

## REFERENCES

[1] R. Nee, and R. Prasad, *"OFDM for Wireless Multimedia Communications"*, Artech House, 2000.

[2] B. Farhang-Boroujeny, "OFDM Versus Filter Bank Multicarrier", *IEEE Signal Processing Magazine,* vol. 28, pp. 92-112, May 2011.

[3] B. Farhang-Boroujeny, "Cosine Modulated and Offset QAM Filter Bank Multicarrier Techniques A Continuous-Time Prospect," *EURASIP Journal on Advances in Signal Processing,* pp. 6, Jan 2010.

[4] V. Ari, B. Maurice, and H. Mathieu, "WP5: Prototype filter and filter bank structure"', *PHYDYAS-PHYsical layer for DYnamic AccesS and cognitive radio,* Jan 2009.

[5] B. Hirosaki, " An analysis of automatic equalizers for orthogonally multiplexed QAM systems," *IEEE Transactions on Communications,* 28(1). pp. 73-83, Jan. 1980.

[6] S. Nedic and N. Popvic, "Per-bin DFE for advanced OQAM-based multicarrier wireless data transmission systems," *Broadband Communications, 2002. Access, Transmission, Networking. 2002 International Zurich Seminar on*, pp. 38-1, Feb. 2002.

[7] D. S. Waldhauser, L. G. Baltar and J. A. Nossek,"MMSE subcarrier for filter bank based multicarrier systems," *Proc. IEEE 9th Workshop on Signal Processing Advances in Wireless Communications*, pp.525-529, July 2008.

[8] A. Ikhlef and J. Louveaux, "An enhanced MMSE per subchannel equalizer for highly frequency selective channels for FBMC/OQAM systems," *Proc. IEEE 10th Workshop on Signal Processing Advances in Wireless Communications*, pp. 186-190. June 2009.

[9] L. G. Baltar, D. S. Waldhauser and J. A. Nossek, "MMSE subchannel decision feedback equalization for filter bank based multicarrier systems," *Proc. IEEE International Symposium on Circuits and Systems* pp. 2802-2805, May 2009.

[10] D. S. Waldhauser, L. G. Baltar, and J. A. Nossek, "Adaptive decision feedback equalization for filter bank based multicarrier systems," *Proc. IEEE International Symposium on Circuits and Systems* pp. 2794-2797, May 2009.